Chapter 4
Biomineralization: Apatite Protein Interaction

Toru Tsuji, Mayumi Iijima, and Kazuo Onuma

Abstract The evolution of recombinant DNA techniques and protein engineering has accelerated the growth in biomineralization studies over the last decade. In this chapter, we discuss recently published work focusing on the structure and function of proteins that are involved in HAP crystal formation in the body. The proteins we focus on in this review are amelogenin and dentin matrix protein 1 (DMP1). The roles of other proteins, for example, SIBLING family members, which are supposed to play significant roles in HAP crystal formation, are also described. These proteins would be involved in different steps of HAP crystal formation, that is, nucleation, growth, and transformation. We also summarize the challenges of regulating crystal growth and elucidating the mechanisms of crystal formation using artificial proteins, which are not attained by using only naturally occurring proteins.

Keywords biomineralization • amorphous calcium phosphate • transformation • hydroxyapatite • biomineralization proteins

T. Tsuji (✉)
Advanced Research Centers, Keio University, 3-14-1, Hiyoshi, Kohoku-ku, Yokohama, 223-8522, Japan
e-mail: toruts2002@yahoo.co.jp

M. Iijima
Asahi University School of Dentistry, Oral Functional Science and Rehabilitation, Dental Materials Science, 1851-1 Hozumi, Mizuho, Gifu, 501-0296, Japan
e-mail: iijima@dent.asahi-u.ac.jp

K. Onuma
National Institute of Advanced Industrial Science & Technology, Central 6, 1-1-1 Higashi, Tsukuba, Ibaraki, 305-8566, Japan
e-mail: k.onuma@aist.go.jp

X.Y. Liu (ed.), *Bioinspiration: From Nano to Micro Scales*, Biological and Medical Physics, Biomedical Engineering, DOI 10.1007/978-1-4614-5372-7_4,

4.1 Overview of Bone and Teeth Biomineralization

The crystalline phase of calcium phosphate that participates in bone formation is the hydroxyapatite (HAP) phase, the most stable calcium phosphate phase under physiological conditions. Bone contains collagen—an organic substance—at a dry weight content of 30–40%. Bone is thus an inorganic-organic hybrid material and is characterized by great elasticity and strength compared to pure inorganic substances. Bone HAP nanocrystals measure 30–50 nm in length, 10–50 nm in width, and 3–5 nm in thickness. HAP crystallizes on the collagen fibrils along the direction in which they extend [1].

Bone is synthesized by osteoblasts, which secrete type I collagen into the extracellular matrix. Collagen molecules self-assemble into insoluble fibers through multiple processes. Since biological fluid is supersaturated with respect to HAP, it is not surprising that calcification occurs ubiquitously in the human body [2]. When calcification first begins, minerals are formed specifically on the collagen fibrils. Two mechanisms have been proposed to explain this phenomenon. The first is that some molecules in biological fluid inhibit non-specific mineral deposition. It has been shown that acidic molecules containing carboxyl, phosphate, or sulfate groups inhibit deposition of calcium phosphate in vitro. The second mechanism is owing to the acidic proteins that possess affinity to collagen. Osteoblasts secrete several types of proteins in addition to collagen. Some are acidic, containing many acidic residues such as aspartic acid (Asp), glutamic acid (Glu), and phosphorylated serine, and have the ability to bind to collagen. The binding of acidic proteins to collagen apparently concentrates the calcium ions by using negatively charged groups, which elevates the degree of supersaturation around collagen. This induces calcium phosphate precipitation on the collagen molecules. These processes occur in the early stages of biomineralization during bone formation. As calcification progresses, osteoblasts are buried in the surrounding minerals. Cells imbedded in the minerals no longer secrete proteins and become osteocytes.

Since the details of tooth formation are discussed in Chap. 5, the process is summarized only briefly here. A tooth consists of three layers of mineralized tissue. Enamel forms the outer layer, dentin forms the middle layer, and cementum forms the inner layer, and they are synthesized by ameloblasts, odontoblasts, and cementoblasts, respectively. Tooth calcification is regulated by proteins secreted into the extracellular matrices. Like osteoblasts, odontoblasts and cementoblasts secrete type I collagen, while ameloblasts secrete mainly amelogenin, but not collagen. More than 90% of the organic phase of enamel consists of amelogenin. Amelogenin is believed to regulate the formation of enamel HAP crystals and their assembly into highly organized structures [3].

Enamel HAP crystals differ from those found in bone, dentin, and cementum in their morphology and size. Enamel HAP crystals do not have a platelet structure but rather forms needle-shaped crystals that extend along the *c*-axis. Enamel HAP crystals are much larger than bone ones, measuring 100–1,000 nm in length, 30–60 nm in width, and 10–30 nm in thickness. Enamel HAP crystals have a

higher crystallinity than bone ones and show a sharp peak when measured by XRD analysis. Enamel is formed from large and highly crystallized HAP crystals that are densely packed.

Enamel has a low organic content. In the early stage of enamel formation, the enamel consists of 30% mineral and 20% organic matrix, primarily amelogenin, while the remaining 50% consists of water. During the maturation process, the amelogenin is degraded by proteolytic enzymes and disappears from the enamel. This results in a final enamel composition of 95–97% inorganic content and less than 1% organic content [4]. Thus, enamel is an extremely hard tissue that consists almost entirely of inorganic substances (the elastic modulus of enamel is 80 GPa, [5] whereas that of bone is 10 GPa [6]). However, enamel does not possess as much flexibility as bone (the tensile strengths of enamel are 10 or 40 MPa according to direction [7], whereas that of bone is 100 MPa [8]).

The proteins secreted into the extracellular matrices play a key role in the mineralization of bone and teeth. Recent observations have shown that, in the early development of both bone and enamel, the minerals comprising them consist of a large amount of amorphous calcium phosphate (ACP) [9–11]. Eventually, HAP crystals form from the ACP and assemble into aggregates, which have structures specific to bone and teeth functions. Therefore, to understand the biomineralization of bone and teeth, it is necessary to know how proteins in the extracellular matrices are involved in the deposition of ACP, the nucleation of nanocrystals, and in the growth, transformation, and formation of hierarchical structures made by comprising aggregates of nanocrystals.

In this chapter, we introduce results from recently published work focusing on the structure and function of proteins that are involved in HAP crystal formation in the body. We also summarize the challenges to regulating crystal growth and elucidating the mechanisms of crystal formation using artificial proteins, which are not attained by using only naturally occurring proteins.

4.2 Proteins Involved in HAP Crystal Formation

The proteins involved in HAP crystal formation can be categorized into three groups on the basis of their functions. Those in one group form the insoluble organic matrix and determine the contours of the hard tissues. Type 1 collagen is the organic matrix for bone, dentin, and cementum, while amelogenin is the matrix for enamel. Those in the second group produce mineral deposits in specific areas. They bind to collagen and accelerate HAP crystallization. Those in the third group inhibit deposition of minerals in inappropriate areas. Since biological fluid is supersaturated with respect to HAP, it is not surprising that depositions take place ubiquitously in the body. Proteins with inhibitory function against non-specific deposition are therefore important for normal tissue formation.

4.2.1 Role of Collagen in Forming Insoluble Matrix

Type 1 collagen determines the shape of bone, dentin, and cementum. Collagen consists of polypeptides known as α-chains. One α-chain consists of approximately 1,000 amino acids, each with a molecular weight (M_w) of about 100,000. Collagen has a high glycine content, which makes up approximately one third of the total amino acid content. Following glycine is proline, which comprises one fifth of the total amino acid content. Some proline and lysine residues are hydroxylated after translation and exist as hydroxyl-proline and hydroxyl-lysine, which are specific for collagen. Each α-chain forms a left handed polyproline II type (PPII) helical coil, and further associates to form right handed triple helix. Each α-chain has a repetitive motif consisting of $(Gly\text{-}X\text{-}Y)_n$ in which glycine repeats at every third amino acid. The structure of the triple helix is maintained by glycine, which has a small side chain, placed inside the helix. The linkage of adjacent α-chains is stabilized through hydrogen bonds linking the amino and carboxyl groups of the backbone of the polypeptides [12, 13].

The collagen is secreted into the extracellular matrix as a protocollagen strand containing propeptides at its N- and C-termini. The strand associates to form procollagen triple helix after post-translation modification of lysine and proline residues. The propeptide domains are cleaved by proteases, producing tropocollagen triple helix, which self-assembles into collagen microfibiril. The microfibiril assembles to be an insoluble collagen fiber. Examination of collagen fibers under an electron microscope reveals striped patterns at 67 nm intervals. Each interval is called a "D-period" and arises from the staggered arrangement of the triple helices. Each space created by this arrangement is called a "gap zone," and this is the area in which mineral deposition occurs. It is believed that extracellular matrix proteins bind to this gap zone and induce mineral deposition [2].

4.2.2 Role of Amelogenin in Forming Insoluble Matrix

Although the amino acid sequence of human amelogenin is known, amelogenin from bovine, porcine, and mouse are primarily used for research purposes. Among these, bovine amelogenin is the longest, with 197 amino acid residues, while porcine amelogenin is the shortest, with 173 amino acid residues [14]. The molecular weight of amelogenin estimated from the amino acid sequence is 20–22 kDa, with an isoelectric point of 6.5. Amelogenin can be divided into three domains on the basis of the properties of the amino acid sequence. The N-terminal domain consists of 45 amino acid residues, and is known as TRAP (tyrosine-rich amelogenin peptide). Serine residues that eventually become phosphorylated are also located in this domain. The proline-rich and hydrophobic middle-core domain has been reported to be responsible for the formation of the PPII structure [15]. The PPII structure is a mild helix structure that can also be seen in collagen, and is often

seen in proteins that do not undergo folding. The C-terminal domain consists of only 11 amino acids, which are charged and hydrophilic. Although amelogenin is an intrinsically disordered (natively unfolded) protein that does not have a defined three-dimensional structure, it self-assembles and forms a β-sheet structure at high concentrations [16]. Details concerning intrinsically disordered proteins are discussed later in this chapter. Although the amelogenin molecule is highly hydrophobic overall, due to the hydrophilic nature of the C-terminal region, it forms an amphiphilic structure and self-assembles into nanospheres with a hydrodynamic radius of 5–50 nm [14]. The nanospheres further aggregate and form a ribbon-like structure on a micrometer scale [17]. It is of great interest to know what role this high level of protein organization plays in the enamel formation process.

4.2.3 Role of SIBLING Protein Family in Extracellular Matrices

The genes for the proteins involved in the crystallization of HAP are clustered on human chromosome 4 [18]. They include dentin sialophosphoprotein (DSPP), dentin matrix protein 1 (DMP1), bovine sialoprotein (BSP), matrix extracellular phosphoglycoprotein (MEPE), osteopontin (OPN), enamelin (ENAM), ameloblastin (AMBN), statherin (STATH), histatin (HYN), proline-rich proteins (PROL), and caseins (CSN). DSPP, DMP1, BSP, MEPE, and OPN are expressed in bone and dentin. These proteins belong to the small integrin-binding ligand N-linked glycoprotein (SIBLING) family since they contain an integrin-binding motif (Arg-Gly-Asp), are small, and are glycosylated [19]. Integrins are receptor proteins on the cell surface that regulate intracellular signaling through the binding of ligands. SIBLING proteins are believed to be involved in mineralization through their interaction with calcium phosphates. They may also be involved in cell signaling through interaction with integrins and other receptor proteins. These proteins may play a role in cancer development [20].

Although their expression level is low, both ENAM and AMBN can be found in enamel, together with amelogenin. STATH, HYN, and PROL are expressed in saliva, while CSN is expressed in milk. The similarity of the exon and intron organization and the repetitive sequences of the genes of these proteins imply that they evolved from a common ancestor protein [21, 22].

Among the SIBLING proteins, DMP1, BSP, and OPN can bind to collagen. DSPP is proteolytically cleaved, resulting in DSP (dentin sialoprotein) and DPP (dentin phosphoprotein or phosphophoryn) products. Among these proteins, DPP is able to bind to collagen. Experiments on HAP crystal formation in the presence of DMP1, BSP, OPN, and DPP showed that these proteins induce crystallization. They most likely have the ability to bind to the collagen gap zone (See note above) and form HAP crystals on collagen fibrils [2].

4.2.4 Structure and Function of Biomineralization Proteins

Ever since the discovery of the DNA double helix structure by Watson and Crick, structural biology has made great contributions to progress in the life sciences. This is because the functions of biopolymers can be inferred from their static structures. In many cases, protein function mechanisms can be understood by revealing their tertiary structures. If a protein does not have such a structure, it is impossible to determine that structure by any means. Many proteins involved in biomineralization do not have such a stable structure, making it difficult to determine a static tertiary structure using X-ray crystallography or nuclear magnetic resonance (NMR) analysis. Proteins that cannot fold into a stable structure are called "intrinsically disordered proteins" or "natively unfolded proteins" [23]. There are about 20,000 genes in the human genome, and approximately 100,000 proteins are synthesized from the genes through mechanisms including alternative splicing, which increase protein diversity. It is suggested that 33% of eukaryotic proteins contain unfolded regions lacking a stable structure [24, 25]. Proteins with unfolded regions are considered advantageous for binding multiple targets or for binding tightly to target compounds [26, 27].

The "lock and key" and the "induced-fit" models were proposed to explain how proteins recognize their substrates. In the "lock and key" model, the protein already has a structure complementary to its substrate. In the "induced fit model," the protein does not have a complementary structure, but formation of one is induced by interaction with the substrate. Common to both models is that the protein itself has a clear stable structure regardless of the experimental conditions, including the presence or absence of a substrate.

In contrast, it has been suggested that natively unfolded proteins can bind to substrates through a mechanism called "conformational selection" [28]. That is, a protein has multiple metastable conformations in the absence of a substrate and fluctuates continuously between the conformations. In the presence of a substrate, a metastable conformation complementary to the substrate is selected, and a complex is formed. The selected conformation becomes the most stable conformation. For example, the ubiquitin polypeptide, consisting of 76 amino acid residues, can form complexes with many different proteins; a total of 46 crystal structures have been reported to date. Analysis of the dynamics of ubiquitin in solution by NMR revealed a group of structures including the 46 crystal structures, thereby validating the concept of "conformational selection" [29].

For proteins involved in biomineralization, one report on statherin is noteworthy. Statherin is a small 43-amino acid protein found in saliva that inhibits the formation and growth of HAP crystals. The C-terminus of statherin does not have an ordered conformation in solution; however, structural analysis using solid-state NMR indicated that the C-terminal domain forms an α-helix upon binding to HAP [30]. The binding of statherin to HAP occurs mainly through charged amino acids at the N-terminus [31, 32], and the interaction of the C-terminus with HAP is not tight

[33]. It is unclear how this structural change in statherin induced by HAP binding can influence affects crystal growth. Schwartz reported that the C-terminal domain of statherin contributes to the inhibition of HAP precipitation [34].

4.3 Controlling Calcium Phosphate Precipitation

Mahamid et al. demonstrated the existence of a large amount of ACP in the early stage of bone formation by analyzing the mineral phase of fin bone formation in zebrafish [10]. Beniash et al. demonstrated the existence of ACP in the early stage of mouse incisor enamel formation [11]. These findings indicate that the first calcium phosphate that appears in bone and enamel is ACP. The hierarchical complex structures seen in bone and enamel are thus initially formed by ACP as a building block, and are organized in a spatiotemporal manner by the aid of proteins in extracellular matrices produced by osteoblasts or ameloblasts. Interaction between the ACP and biomolecules is discussed in this chapter.

As described above, since extracellular fluid is supersaturated with respect to HAP, it is not surprising that deposition takes place ubiquitously in the human body. However deposition in unsuitable areas is strictly controlled so that hard tissues are formed properly. For example, acidic biomolecules inhibit deposition of calcium phosphate in vitro. Acidic functional groups such as phosphoryl, carboxyl, and sulfate groups bind and chelate calcium ions, which reduce the concentration of calcium ions and the degree of supersaturation in body fluids. For example, the C-terminus of amelogenin, which is expressed in the early stage of enamel development, is proteolytically cleaved resulting in a P148 protein consisting of 148 amino acid residues [35, 36]. P148 is a major component of the organic matrix in enamel; it inhibits the deposition of ACP when it is phosphorylated [37].

One detailed mechanism of the inhibitory effects of the deposition of calcium phosphate has been proposed. DMP1, an acidic protein with a molecular weight of 50,000, is a SIBLING protein. Like many other proteins involved in biomineralization, DMP1 does not have an ordered backbone conformation [38]. However, in the presence of Ca^{2+}, a secondary structure suitable for self-assembly is formed. In this formation, the proteins aggregate into microfibrils [39]. Atomic force microscope (AFM) and transmission electron microscope (TEM) measurements revealed that complexes were formed by the combining of DMP1 oligomers and calcium phosphate particles. DMP1 oligomers were shown to inhibit mineral deposition, apparently by binding to the mineral particles and sequestering them from the external solution [40]. DMP1 has the ability to bind collagen, and, in the presence of collagen, accelerates HAP crystal formation [41]. On the basis of several observations, He et al. proposed a model in which DMP1 oligomers bind to calcium phosphate particles, thereby preventing nonspecific deposition. DMP1 binds to suitable areas of the collagen fiber in the extracellular matrix and induces calcification at specific sites (Fig. 4.1, [40]).

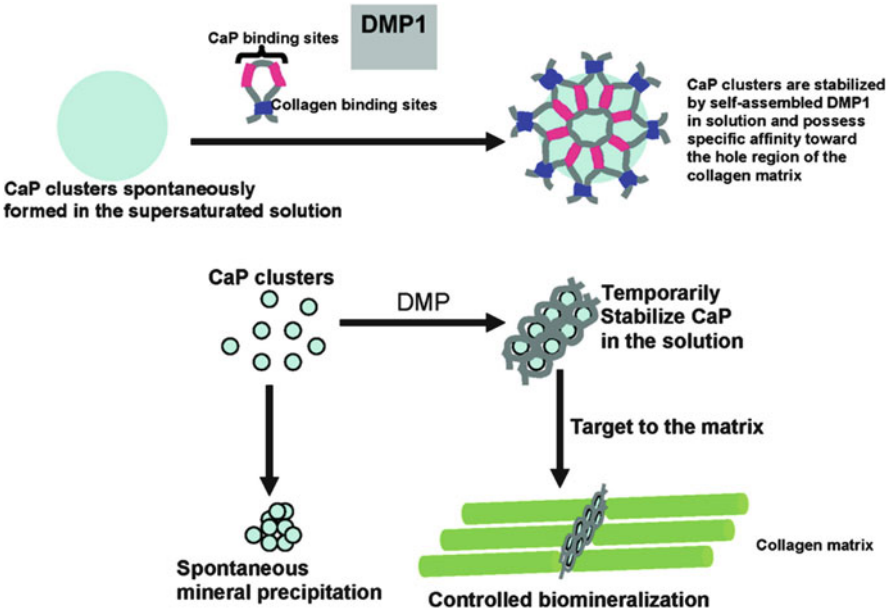

Fig. 4.1 Proposed function of DMP1. DMP1 self-assembles to the oligomeric state and inhibits spontaneous precipitation by sequestering calcium phosphate clusters from external solution. Binding of the protein to collagen fibers promotes nucleation of apatite in the matrix. Reprinted with permission from [40]. (Copyright 2005, American Chemical Society)

In addition to hard tissues such as bone and teeth, body fluids including saliva, milk, and urine are supersaturated with respect to HAP. When calcification occurs in blood vessels, it causes arteriosclerosis. Therefore, a mechanism to prevent calcium phosphate deposition in body fluid is needed for soft tissues. Fetuin forms a complex with calcium phosphate, which prevents mineral deposition [42, 43]. In milk, casein and osteopontin form a complex with calcium phosphate and further form micelles, resulting in prevention of mineral deposition in serum. In vitro experiments using a phosphorylated form of a 25 amino acid peptide, derived from the casein sequence, showed that ACP clusters with a radius of 2.4 nm were covered by peptide molecules with a thickness of 1.6 nm [44, 45]. A phosphorylated form of an osteopontin-derived peptide also binds to ACP clusters, forming a complex that prevents calcium phosphate precipitation [46].

In some cases, deposition of ACP is promoted. Poly-lysine and poly-glutamic acid (basic and acidic polymers with an isoelectric point (p*I*) of 10.5 and 4.9, respectively) were added to a calcium phosphate solution supersaturated with respect to ACP. Deposition of ACP was accelerated at a low concentration of either polymer, and deposition was delayed at a high concentration. Although the detailed molecular mechanisms of this acceleration and inhibition is are unknown, it was found that, regardless of negative or positive charge, mineral deposition is either accelerated or inhibited in a dose-dependent manner regardless of the polymer's charge [47].

4.4 Controlling Nucleation and Aggregation of HAP or OCP

Mouse amelogenin (composed of 179 amino acids), which is involved in enamel formation, was expressed in *Escherichia coli* using a recombinant DNA technique. When recombinant mouse amelogenin (rM179) was mixed in a calcium phosphate solution, which is supersaturated with respect to HAP and OCP, OCP formation was accelerated [48]. Nucleation of crystals occurs when the thermodynamic driving force of the crystal phase overcomes the negative effect of the surface free energy of small particles. If a part of the atomic arrangement of rM179 is complementary to the OCP crystal faces, the binding of rM179 to calcium phosphate particles reduces the surface free energy of the particles, which induces heterogeneous nucleation of the OCP. This heterogeneous nucleation apparently accelerates OCP precipitation. The amount of OCP precipitated depends on the rM179 concentration. The maximum amount of OCP was precipitated at an rM179 concentration of 6.5 μg/mL, and OCP deposition decreased as the rM179 concentration was increased. This was explained as follows: an increased amount of rM179 results in more binding of calcium and phosphate ions to the protein, which reduces the degree of solution supersaturation.

Moreover, rM179 not only accelerates nucleation but also regulates the assembly of HAP crystals. To investigate the function of the charged C-terminal domain of amelogenin, Beniash et al. generated rM166, which lacks the C-terminal domain of rM179. Crystallization experiments were performed in the presence of these proteins, and the properties of the resultant crystals were compared [49]. The HAP crystals that formed in the presence of rM179 were bundle-like aggregates aligned with the *c*-axis and were organized in a manner similar to the HAP in enamel. Those that formed in the presence of rM166 assembled into aggregates with a random orientation. This indicates that the C-terminal domain of amelogenin is essential for ordered assembly of HAP crystals. When pre-aggregated amelogenin was added to supersaturated solution, The HAP crystals aggregated with a random orientation, and aggregates aligned along the *c*-axis were not obtained. This suggests that the self-assembly of amelogenin and the organization of HAP crystals proceed in a cooperative manner.

Wang et al. expressed full-length recombinant porcine amelogenin (rP172) in *E. coli* and investigated the effect of the protein on crystallization and crystalline calcium phosphate aggregation. Spherical aggregates of OCP crystals were formed in the absence of rP172, and HAP crystal aggregates aligned along the *c*-axis formed in its presence. The induction time for nucleation decreased as the concentration of amelogenin was increased (measured in the concentration range of 0.5–5.0 μg/mL; maximum acceleration took place at 5 μg/mL).

In addition to the decreased induction time for nucleation, HAP and not OCP was obtained, suggesting the presence of structural matching at the interface between atomic arrangements of the amelogenin surface and HAP crystal faces ([50]; A role of amelogenin proposed by Wang et al. was also described in Sect. 5.4.4 in Chap. 5). This suggestion is based on the theory that the nucleation energy barrier decreases

and the HAP nucleation rate increases when structural matching between HAP and amelogenin takes place. It has been proposed that aligned crystals tend to be formed more often at a lower degree of supersaturation [51, 52].

A future objective is to elucidate the effect of amelogenin on the aggregation of HAP crystals aligned along the *c*-axis. Yang et al. proposed a model regarding the interaction between amelogenin and nanoclusters of calcium phosphate [53]. This model will be described in detail in Chap. 5.

As described above, Tarasevich et al. accelerated OCP deposition using mouse amelogenin, while Wang et al. formed HAP using porcine amelogenin under supersaturated conditions with respect to both HAP and OCP. In both cases, amelogenin-induced heterogeneous nucleation accelerated crystallization. Does mouse amelogenin structurally match OCP, whereas porcine amelogenin structurally matches HAP? Why did porcine amelogenin fail to form HAP deposits? And why did mouse amelogenin fail to form OCP deposits? To understand the template effect of the proteins, it is necessary to analyze the effect of various protein templates under uniform experimental conditions.

4.5 Controlling Crystal Growth

As described in Chap. 3, by analyzing step velocities on the growing crystal face in the presence or absence of different proteins, the effect of these proteins on crystal growth can be quantitatively evaluated. However, such an attempt has not been achieved with HAP. In this section, we describe the effect of amino acids, peptides, and proteins on the growth of calcite, one of the crystal phases of calcium carbonate.

In general, when an impurity adsorbs to a crystal surface, the incorporation of the crystal unit at the kinked site is inhibited, and the growth of the crystal face is slowed. It was found, however, that acidic proteins extracted from pearl layers of abalone, APα and APβ, accelerated crystal growth. Although these proteins were originally extracted from aragonite layers, their effects on the crystal growth were investigated using calcite (104) surface [54].

Elhadj et al. focused on aspartic acid residues in acidic proteins, and quantitatively analyzed the effects of aspartic acid polypeptides (monomers to hexamers (Asp1, Asp2, Asp3, Asp4, Asp5, Asp6)) on crystal growth of the calcite surface by using AFM [55]. The calcite (104) surface consisted of an acute step and an obtuse step, and the step velocities were increased in the presence of peptides. Peptides containing a large number of aspartic acid residues resulted in increased acceleration of crystal growth, and the effect was dose dependent. All peptides accelerated crystal growth at a concentration of less than 1 μM, and inhibited growth at high concentrations. Interestingly, each peptide exhibited step specificity for the acceleration. The growth of the acute step was affected by Asp1 and Asp2, and that of the obtuse step was affected by Asp3 to Asp6. The interaction between calcium atoms and peptides on the calcite surface indicates that the interaction between Asp3

to Asp6 and the acute step is strong, so these peptides should accelerate the velocity of the acute step preferentially. However, when the crystal unit is incorporated into the crystal surface, the structured water that binds to the crystal surface and crystal unit must be removed. Calculations using a semi-empirical quantum mechanical model revealed that when Asp3 to Asp6 is used, more water molecules on the crystal surface at the acute step must be removed**.** This indicates that they more effectively accelerate growth in the obtuse step.

Elhadj et al. also analyzed the effect of various Asp-containing peptides and proteins on the step velocity of a growing calcite face (104) [56]. Growth was accelerated with all molecules at low concentrations (Fig. 4.2). Examination of the acceleration rate and net molecular charge of the individual peptides revealed a clear correlation between the degree of net molecular charge and the crystal growth rate; however, the correlation was not perfect. For example, the AP7-N (aragonitic protein N-terminal domain molecular weight 7 kDa; [57]), which contains many hydrophobic amino acids, deviates from this correlation. This indicates that, in addition to the net molecular charge, the degree of hydrophilicity and hydrophobicity of the additives also affects the crystal growth rate. In fact, when the hydrophilicity–hydrophobicity of peptides used for the experiment was measured and compared with the crystal growth rate, a clear correlation was obtained. The hydrophilic molecules apparently enhanced the dehydration of the crystal face and crystal unit and thereby accelerated crystal growth.

Osteopontin is involved in the crystal growth of calcium oxalate monohydrate (COM) as well as of HAP [58]. COM is a component of kidney stones. Since urine is supersaturated with respect to COM, kidney stones are formed if COM deposition and kidney stone growth are not regulated. Osteopontin is one of the proteins that possess this inhibitory function. Grohe et al. derived peptide-containing phosphorylated serines and acidic amino acids (pSHEpSTEQSDAIDpSAEK) from the osteopontin sequence and prepared three synthetic peptides—one with three phosphates (P3), one with one phosphate (P1), and one with no phosphates (P0)—and investigated their interaction with COM [59]. All three peptides adsorbed to the COM (100) surface and inhibited crystal growth, with stronger inhibitory effects seen as the number of phosphates increased. Simulation using molecular dynamics showed that the binding to the (100) surface was achieved in the order of P3, P1, and P0. The Asp-12 and Glu-15 of the C-terminus of the P0 peptide were separated from the crystal surface upon binding. The P1 peptide as a whole was close to the crystal surface; however, amino acids from Gln-7 to Asp-12 in the middle of the peptide were slightly distant from the surface. All amino acids in the P3 peptide were close to the crystal surface. The amino acids in the P1 and P3 peptides closest to the crystal surface were aspartic acids and glutamic acids, but not phosphorylated serines. Grohe et al. suggested that the phosphate group has the ability to stabilize the interaction of crystals and peptides by drawing entire peptide molecules to the crystal surface [59]. When crystals were grown in the presence of P3 and P1 peptides, the COM crystal morphology was transformed into a dumbbell shape. P0 does not affect the morphology [60].

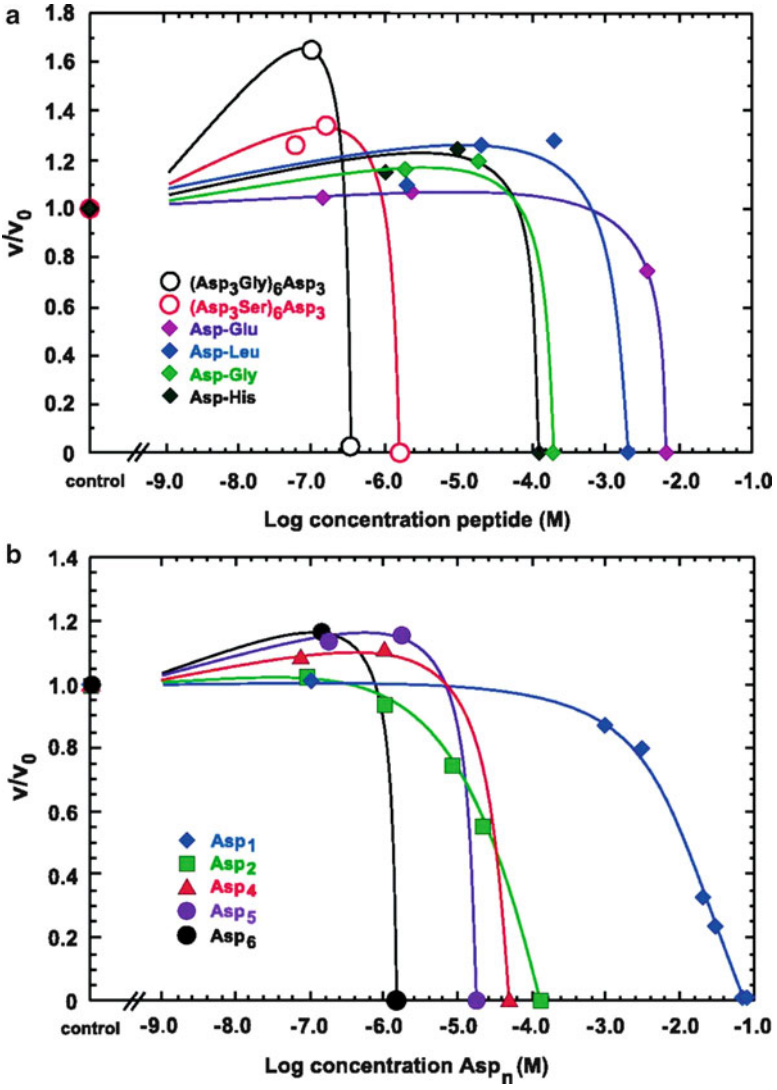

Fig. 4.2 Effects of Asp-containing peptides at different concentrations on obtuse step velocity on calcite (104) face. Dipeptides and 27-mer peptides (a) and aspartic acids of increasing molecular size (b) were used. v and v0 are step velocities in presence and absence of peptides, respectively. Reprinted with permission from [56]. (Copyright 2006, National Academy of Sciences of the United States of America)

Analysis of the interaction of COM and full length osteopontin was also performed [61]. Osteopontin obtained from cow's milk (mOPN) contains 25 phosphorylated residues, whereas osteopontin from rat's bone (bOPN) contains 10 phosphorylated residues. The binding effects to COM of these phosphorylated

proteins, as well as recombinant rat osteopontin (rOPN) lacking phosphate residues, were compared. All three OPN proteins adsorbed to the edge of the (100) and (121) surfaces of the COM crystals. However, only the mOPN and bOPN changed the crystal morphology to a dumbbell shape. The rOPN lacked this morphological transforming ability.

The attachment of mOPN and bOPN to the COM crystal surface was investigated in detail [62]. The adsorption of mOPN was more specific to the (100) surface. Since the (100) surface of COM is the richest surface in terms of calcium atoms [63], Langdon concluded, on the basis of the electrostatic interaction between phosphate residues of OPN and calcium ions on the crystal surface, that the adsorption of phosphorylated OPN is not due to the specific structure defined by the amino acid sequence but to a non-specific interaction [62].

The interaction of amelogenin to a specific crystal surface of OCP has been studied [64, 65] and is described in Chap. 5.

4.6 Controlling Transformation

He et al. examined the change in the mineral phase during HAP formation with DMP1 and identified the peptide sequences in DMP1 particularly important for HAP crystal formation. When DMP1 adsorbed to a glass plate was placed in a calcium phosphate solution, ACP precipitated on the glass plate and then transformed into HAP. In a control experiment with bovine serum albumin adsorbed to the glass plate, HAP crystal formation was not observed under the same conditions although a small amount of ACP precipitated. He et al. further found that HAP crystal formation accelerated when two peptides derived from DMP1 (ESQES and QESQSEQDS) were adsorbed to the glass plate, as seen with DMP1 [39]. However, the mechanism of HAP crystal formation promoted by the protein or peptides was not determined. Tsuji et al. used the same two peptides and applied the experiments to elucidate the mechanism of HAP crystal formation promoted by proteins containing the peptide sequences [66].

The time-resolved static light scattering (TR-SLS) measurement technique developed by Onuma et al. is an excellent method for analyzing the crystallization of small particles freely diffused in solution [67]. This technique enables real-time analysis of the apparent molecular mass, gyration radius, and fractal dimension (an index of the inner structure ordering) of calcium phosphate particles. However, although DMP1 and peptides ESQES and QESQSEQDS accelerate crystal formation when they are adsorbed to insoluble matrices such as collagen or a glass plate [38, 39], they do not accelerate crystal formation when they are present in a free form [40]. Thus, the mechanism of HAP crystal formation induced by DMP1 and these peptides cannot be analyzed using TR-SLS measurement.

Therefore, an attempt was made to synthesize proteins that can accelerate HAP crystal formation without immobilization. In general, there are strict limitations on the design and production of proteins with a desired function using only

knowledge of the structure–function relationship. Since current knowledge on the structure–function relationship of proteins is incomplete, it is more practical to take a combinatorial approach [68–70]. Using a motif programming method [71], Tsuji et al. generated a combinatorial library of proteins containing peptides ESQES and QESQSEQDS in various numbers and different orders. Eighteen genes were synthesized in vitro, expressed in *E. coli*, and purified using affinity chromatography. Proteins with the ability to accelerate HAP crystal formation without immobilization were then identified. A calcium phosphate solution with an adjusted pH of 7.4 did not produce deposits within a 10-day reaction time. Adding 1.6 μg/mL of artificial protein (#64) led to the formation of spherical aggregates of OCP within 5 days. In crystallization experiments using supersaturated solution with a high pH (8.0), #64 protein accelerated HAP crystal formation. The process of HAP crystal formation in the presence of #64 protein was analyzed using TR-SLS measurements [66].

As a control, a crystallization experiment was performed in the absence of the protein. Upon mixing of phosphate and calcium solutions, particles with a gyration radius of 350 nm soon formed. The fractal dimension of the initial phase was small (1.8). TEM analysis showed that the particles had a rounded morphology, and only a diffusive ring was observed by selected area electron diffraction (SAED), indicating that the initial particles were ACP. The initial state was maintained for 90 min. After additional time had elapsed, the apparent molecular mass, gyration radius, and fractal dimension increased simultaneously, and HAP crystal formation occurred. In the presence of protein #64 (1 μg/mL), the initial particles were ACP with a gyration radius of 350 nm, similar to that of those obtained in the absence of the protein. In contrast to a situation on a control experiment, the apparent molecular mass and fractal dimension increased after 80 min, and HAP crystal formation was achieved.

It is important to note the differences in the transformation mechanisms. While the apparent molecular mass, gyration radius, and fractal dimension increased simultaneously in the absence of the protein, only the apparent molecular mass and fractal dimension increased and the gyration radius remained unchanged in the presence of the protein (Fig. 4.3). This indicates that, in the presence of the protein, ACP particles are transformed into crystals without a change in their size. In other words, the rearrangement of atoms or clusters takes place within the ACP particles during their transformation to HAP crystals. This transformation mechanism is known as direct transformation [67]. During the transformation process of ACP to HAP, artificial proteins containing peptide sequences derived from DMP1, as designed by the motif programming method, accelerate HAP crystal formation by altering the mode of the transformation to direct transformation [66].

Is direct transformation actually taking place inside the body? Beniash et al. studied enamel formation in mouse incisor [11]. They found that different developmental stages exist in different areas simultaneously, so it is suitable to identify the mineral phase at each developmental stage. When enamel was stained with toluidine blue dye, the staining pattern of the immature outer enamel differed

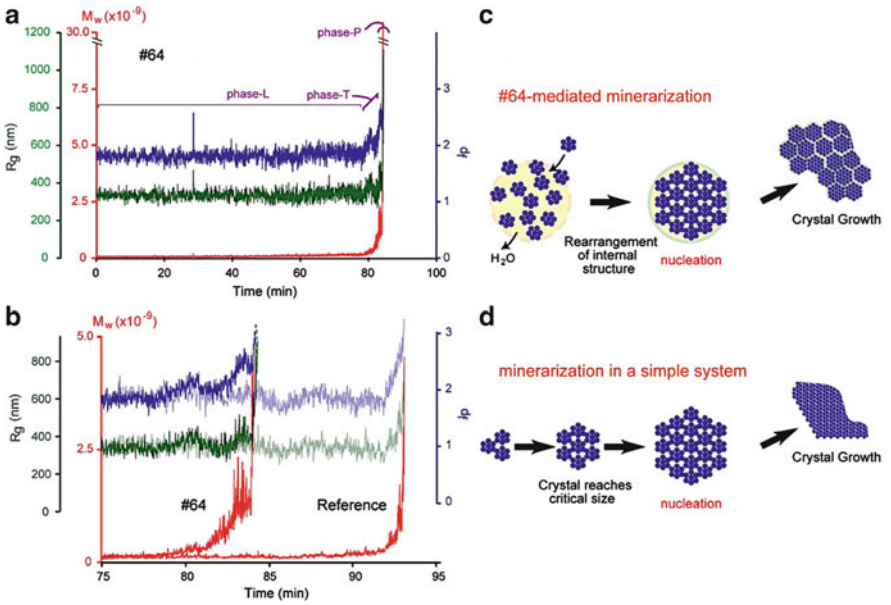

Fig. 4.3 Results of TR-SLS measurement of calcium phosphate formation. (a) Time-dependent changes in calculated apparent molecular mass (M_w, red), gyration radius (R_g, green), and fractal dimension (d_f, blue) of calcium phosphate in presence of artificial protein (#64, 1 μg/mL). Phase L (latency) was followed by phase T (transformation), and phase P (precipitation). (b) Enlargement corresponding to 75–95 min in (a). For comparison, the data obtained in the absence of #64 are shown in light colors. (c and d) Schematic representations of HAP mineralization via direct transformation mediated by a protein (c) and in a simple system (d). Reprinted with permission from [66]. (Copyright 2008, National Academy of Sciences of the United States of America)

from that of the mature inner enamel. This was attributed to the compositional differences between the organic substances in the various areas resulting from protein degradation during the enamel maturation process [72].

Observation of these areas using polarizing microscopy revealed birefringence only in the inner area. In other words, immature outer enamel does not contain crystals. Observation of sections from these areas by TEM revealed needle-shaped mineral crystallites arranged in parallel arrays, the typical morphology of enamel. The crystallites were several nm thick, 20 nm wide, and several hundred nm long, and there was no significant variation in their shape or size. There was, however, a significant difference in their patterns of electron diffraction. Those in the inner area showed 002, 004, 112, and 311 diffraction patterns, which are characteristic for HAP, whereas those in the outer area exhibited a broad ring, which is a typical pattern for ACP. In other words, the degree of crystallization differed between the inner and outer areas although the sizes and morphologies of the crystallites were similar. This suggests that transformation from ACP to HAP is not caused

by the growth of particles. Rather, the inner area minerals were crystallized by rearrangement of the atoms or clusters inside the particles [11]. This means that the apatite of enamel is formed from ACP by direct transformation.

The artificial protein used in the TR-SLS experiment by Tsuji et al. contained peptide motifs derived from DMP1. These motifs are expressed in bone and dentin but not in enamel. It would be of interest to examine the mode of crystallization by using the TR-SLS measurement technique and an enamel-specific protein such as amelogenin. As described in the previous section, amelogenin, unlike DMP1, induces HAP deposits without immobilization. This means that it can be simply applied to SLS measurements. It would also be worthwhile to obtain information on the crystallization of bone and dentin through in vivo observations.

An important study by Beniash et al. found that, not only the size and shape, but also a high level of structural organization is formed before the phase transformation from ACP to HAP [11]. This suggests that the body possesses mechanisms for constructing hierarchical structures by controlling the organization of ACP particles.

Tao et al. observed that organic molecules can control the hierarchical assembly of HAP by using ACP particles as building blocks [73]. HAP is formed by mixing calcium and phosphate ions in the presence of poly(acrylic acid) (PAA). Under these conditions, HAP spheres measuring 5 nm in diameter were formed. The PAA enables apatite spheres to stably exist without growing or assembling. High-resolution transmission electron microscope (TR-TEM) observation revealed that these particles consist of a 5 nm HAP core and an ACP shell. When the PAA was removed, the HAP particles formed colloidal aggregates. Even under colloidal conditions, the layered structure of the HAP core and ACP shell was maintained, and the particles were linked via ACP regions. SAED showed diffraction rings, meaning that the particles were nanocrystalline aggregates packed with a random orientation. The aggregates were 30 nm in size. When colloidal particles were dispersed in water in the presence of biological additives, they re-assembled into highly ordered structures. Needle-shaped single crystals and plate-like single crystals formed in the presence of Gly (glycine) and Glu (glutamic acid), respectively.

These structures are formed in the following manner. In the presence of Gly, core-shell aggregates line up. These aggregates are connected by ACP. At this stage, the direction of the HAP core of each aggregate is random. Since ACP is unstable and is transformed into HAP, the structures of connected regions of the aggregates shift from HAP-ACP-HAP to HAP-HAP-HAP. Since ACP has a fluid-like character, the HAP core within the ACP shell can rotate into the most stable orientation. Simultaneous rotation of the HAP core and transformation from ACP to HAP at the junction site results in alignment of adjacent HAP, which stabilizes the overall structure. Aggregates of nanospheres with the same orientation are thereby formed and become needle-like single crystals of HAP. This formation of needle-like single crystals takes approximately 10 days. Because the crystals are still surrounded by an ACP shell, they aggregate further. Thus, micrometer-sized HAP crystals resembling enamel HAP crystals are formed. The formation of the HAP crystals takes approximately 2 months.

A similar high level of organization was seen in the presence of amelogenin as well. Surprisingly, while 2 months were required to form this high level of organization in the presence of Gly, the process completed in only 3 days in the presence of amelogenin. This accelerated formation of needle-like aggregates of HAP crystals parallel to the *c*-axis mediated by amelogenin was reported by several groups [49, 50, 53]. This characteristic of amelogenin was confirmed in an experiment using HAP core-ACP shell particles.

On the other hand, in the presence of a Glu, HAP core—ACP shell particles were seen to reorganize into a different type of hierarchical structure and form a plate-like single crystal with a large surface (0001), which resembled the HAP crystals found in bone. In a control experiment, no highly organized structure was formed even with the addition of Glu, Gly, or amelogenin when pure HAP crystal particles without an ACP shell were used.

Although several experiments showed crystal formation due to the aggregation of nanocrystals [73, 74], the one by Tao et al. showed something particularly important: ACP connects HAP at the different crystal surfaces and forms various hierarchical structures depending on the condition of various biomolecules. Biomolecules added to the reaction determine the assembly orientation of the nanocrystals and accelerate the aggregation and transformation.

The role of Gly and Glu in the control of the morphology of nanocrystal aggregates was clarified using molecular dynamics simulation. The interfacial energies of the (0001) face and the $(1\bar{1}00)$ face of HAP in water are similar. The effects of Gly and Glu adsorption on these faces on their interfacial energies were examined. Adding Gly markedly raised the energy of the (0001) face and slightly reduced that of the $(1\bar{1}00)$ one. Thus, HAP (0001) faces become unstable in Gly solution, resulting in packing on the (0001) face and formation of a hierarchical structure along the *c*-axis. In contrast, simulation showed that the (0001) face is significantly stabilized by Glu while the $(1\bar{1}00)$ face is not affected. This indicates that packing takes place at the $(1\bar{1}00)$ face, resulting in aggregation along the axis vertical to the *c*-axis, with preferential formation of a plate-like superstructure. The simulation results explain the experimental observations, i.e., formation of needle-like HAP crystals and plate-like HAP crystals with Gly and Glu, respectively (Fig. 4.4).

4.7 Controlling Mineralization with Artificial Proteins and Peptides

An important molecular biological method is display technology. Typical display technologies include phage display [75], cell surface display [76], ribosome display [77], and mRNA display [78, 79]. Among these, phage display and cell surface display have been widely used and have been applied to inorganic materials [80]. A phage is a virus that infects *E. coli* and has a structure in which its genome is

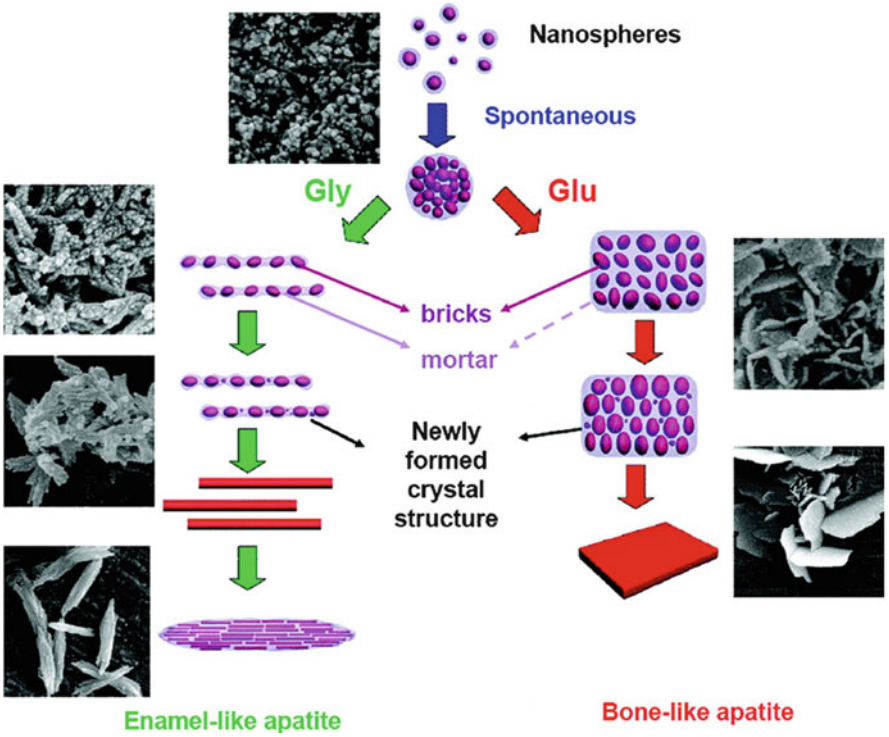

Fig. 4.4 Model of hierarchical assembly of apatite nanocrystals mediated by glycine and glutamic acid. Nanocrystals consisting of HAP core (purple) and ACP shell (light blue) aggregated spontaneously and were dispersed in water. In the presence of indicated amino acids, nanocrystals reassembled into different hierarchical structures. One-dimensional linear assemblies and two-dimensional plate-like structures were formed in the presence of Gly and Glu, respectively. Nanocrystals were connected by ACP surrounding HAP core. ACP transformed into thermodynamically stable HAP, and, at the same time, HAP core rotated to the most stable orientation. As a result, each HAP domain had the same crystallographic orientation and fused into single crystals. Reprinted with permission from [73]. (Copyright 2007, American Chemical Society)

encapsulated within a membrane consisting of proteins. When a gene encoding an artificial peptide is inserted into a gene encoding a membrane protein using recombinant DNA technology, a chimeric protein consisting of the membrane protein and the peptide is synthesized and displayed on the surface of the phage. If the artificial peptide has the ability to bind to the target compound, the phage will also be able to bind to that compound.

DNA sequences encoding 12–16 amino acids are usually inserted into a membrane protein gene. In a typical experiment, up to 10^9 phages displaying 10^9 different peptide sequences can be used. First, 10^9 phages and the target compound are mixed together. Phages that have affinity to the target compound are recovered using an affinity chromatography-like technique. The recovered phages are infected

with *E. coli* and propagated. Their DNA and peptide sequences are then determined. The concept of cell surface display is essentially the same. Cells bound to the target compound are collected and propagated, and genes encoding the peptides with binding activity are obtained.

Although display technology is commonly used in the molecular biological field for identifying the interaction of biomacromolecules such as proteins and/or peptides, it has also been used to recover peptides that bind to gold. Brown, for example, used cell surface display to recover peptides that bind to gold and showed that such peptides can be used to control gold crystal formation [81, 82]. Since then, display technology has been applied to research in the field of material science and used to synthesize semiconductor crystals [80, 83–85]. Mao et al. successfully fabricate zinc blende and Wurtzite ZnS crystal systems using two kinds of artificial peptides. The zinc blends structure was obtained in the presence of a peptide, and the Wurtzite ZnS structure was obtained in the presence of another peptide.

Peptides that bind to HAP have been isolated using phage display. Gungormus et al. used it for crystallization experiments in which two artificial peptides, a HAP strong-binding peptide (HABP1, CMLPHHGAC) and a HAP weak-binding peptide (HABP2, CNPGFAQAC), were added to supersaturated solutions with respect to HAP and OCP. Only OCP was obtained in the presence of both peptides. Both peptides delayed OCP formation, with more drastic effects seen in the presence of HABP1. The OCP crystals obtained in the presence of HABP1 were significantly larger than those obtained in the presence of HABP2 [86].

Roy et al. used phage display to isolate a peptide that binds to HAP [87]. The peptide contained the amino acid sequence SVSVGMKPSPRP. It bound efficiently to HAP, but did not bind to ACP or calcium carbonate, indicating that the peptide recognize HAP-specific atomic sequences, and not calcium or phosphate ion ones. Roy et al. showed that the peptide modified with fluorescent dye can be used for imaging teeth. The use of this technology should make it possible to analyze the processes of bone and teeth development with high sensitivity in vivo.

A peptide that can bind to titanium, commonly used for artificial bone, was isolated using phage display [88]. Although titanium has good biocompatibility, it does not bind to bone directly. Therefore, patients receiving a titanium implant are generally obliged to restrict mastication for several weeks until tight adhesion between the implant and surrounding bone is established. To overcome this problem, methods to accelerate the adhesion process have been investigated. Bone is synthesized by osteoblasts, and bone morphological protein 2 (BMP2) induces differentiation of premyoblastic cells into the osteoblastic state. Therefore, it may be possible that BMP2 immobilized on a titanium substrate induces cell differentiation into osteoblastic state, which promotes tight adhesion between the titanium substrate and surrounding bone. However, when BMP2 is directly attached to a titanium surface, it becomes inactivate due to inappropriate interaction between the protein and titanium surface. To overcome this problem, an artificial protein that binds tightly to titanium was constructed using the titanium binding peptide as a building block. The artificial protein was fused to BMP2, and the BMP2 was attached to a

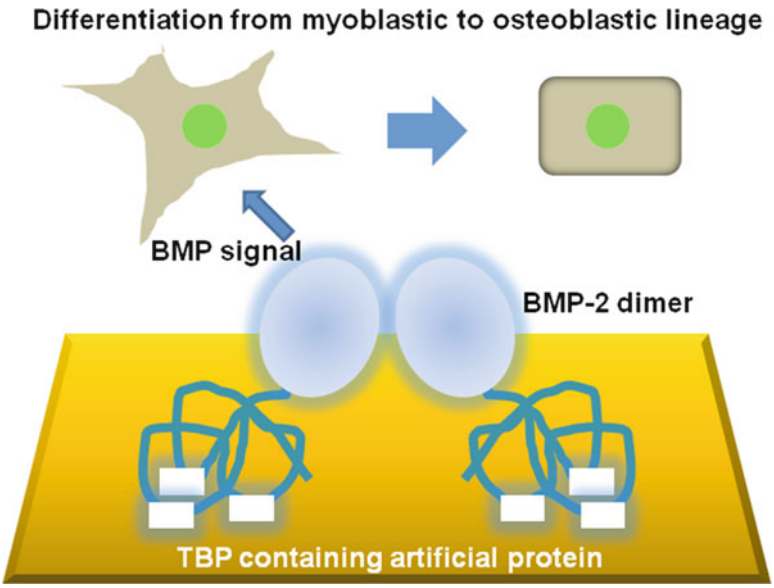

Fig. 4.5 BMP2 fused to artificial proteins containing titanium binding peptides were immobilized on titanium surface. Artificial proteins could associate with titanium surface in a reversible manner, enabling them to be BMP2 with an active state. Reprinted with permission from [89]. (Copyright 2009, Elsevier)

titanium surface using the artificial protein. Indeed, Kashiwagi et al. observed BMP-induced differentiation of osteoblastic cells when myoblastic cells were cultivated on a BMP2-modified titanium surface (Fig. 4.5, [89]).

Tsuji et al. created an artificial protein by combining DMP1-derived peptides and a titanium-binding peptide. The resulting protein showed bifunctionality—titanium binding activity and nucleation activity of crystalline calcium phosphate-, and could be used for coating of a titanium surface with OCP film under biologically relevant conditions [90]. The use of OCP coated titanium for implants would accelerate adhesion between the implants and surrounding bone.

4.8 Closing Remarks

In this chapter, we summarized the results of various research studies pertaining to biomineralization related to HAP crystal formation from the viewpoint of protein science and protein engineering. The utilization of protein and peptide engineering technology should make it possible to control biomineralization at the molecular as well as at the cellular level. Additional proteins with the capability of controlling or affecting biomineralization will likely be constructed. Understanding

the mechanisms of such proteins in detail is important for using them to produce structures with a higher level of organization. Combining technologies for protein structure and dynamics analysis, protein and peptide engineering, and crystal growth analysis will deepen our understanding of biomineralization.

References

1. LeGeros, R.Z.: Calcium phosphate-based osteoinductive materials. Chem. Rev. **108**, 4742–4753 (2008)
2. George, A., Veis, A.: Phosphorylated proteins and control over apatite nucleation, crystal growth, and inhibition. Chem. Rev. **108**, 4670–4693 (2008)
3. Fincham, A.G., Moradian-Oldak, J., Simmer, J.P.: The structural biology of the developing dental enamel matrix. J. Struct. Biol. **126**, 270–299 (1999)
4. Smith, C.E.: Cellular and chemical events during enamel maturation. Crit. Rev. Oral Biol. Med. **9**, 128–161 (1998)
5. Habelitz, S., Marshall, S.J., Marshall Jr., G.W., Balooch, M.: Mechanical properties of human dental enamel on the nanometer scale. Arch. Oral Biol. **46**, 173–183 (2001)
6. Rho, J.-Y., Tsui, T.Y., Pharr, G.M.: Elastic properties of human cortical and trabecular lamellar bone measured by nanoindentation. Biomaterials **18**, 1325–1330 (1997)
7. Giannini, M., Soares, C.J., de Carvalho, R.M.: Ultimate tensile strength of tooth structures. Dent. Mater. **20**, 322–329 (2004)
8. Bayraktar, H.H., Morgan, E.F., Niebur, G.L., Morris, G.E., Wong, E.K., Keaveny, T.M.: Comparison of the elastic and yield properties of human femoral trabecular and cortical bone tissue. J. Biomech. **37**, 27–35 (2004)
9. Gower, L.B.: Biomimetic model system for investigating the amorphous precursor pathway and its role in biomineralization. Chem. Rev. **108**, 4551–4627 (2008)
10. Mahamid, J., Sharir, A., Addadi, L., Weiner, S.: Amorphous calcium phosphate is a major component of the forming fin bones of zebrafish: Indications for an amorphous precursor phase. Proc. Natl. Acad. Sci. U.S.A. **105**, 12748–12753 (2008)
11. Beniash, E., Metzler, R.A., Lam, R.S., Gilbert, P.U.: Transient amorphous calcium phosphate in forming enamel. J. Struct. Biol. **166**, 133–143 (2009)
12. Kadler, K.E., Holmes, D.F., Trotter, J.A., Chapman, J.A.: Collagen fibril formation. Biochem. J. **316**, 1–11 (1996)
13. Shoulders, M.D., Raines, R.T.: Collagen structure and stability. Annu. Rev. Biochem. **78**, 929–958 (2009)
14. Margolis, H.C., Beniash, E., Fowler, C.E.: Role of macromolecular assembly of enamel matrix proteins in enamel formation. J. Dent. Res. **85**, 775–793 (2006)
15. Delak, K., Harcup, C., Lakshminarayanan, R., Sun, Z., Fan, Y., Moradian-Oldak, J., Evans, J.S.: The tooth enamel protein, porcine amelogenin, is an intrinsically disordered protein with an extended molecular configuration in the monomeric form. Biochemistry **48**, 2272–2281 (2009)
16. Lakshminarayanan, R., Yoon, I., Hegde, B.G., Fan, D., Du, C., Moradian-Oldak, J.: Analysis of secondary structure and self-assembly of amelogenin by variable temperature circular dichroism and isothermal titration calorimetry. Proteins **76**, 560–569 (2009)
17. Moradian-Oldak, J., Du, C., Falini, G.: On the formation of amelogenin microribbons. Eur. J. Oral Sci. **114**, 289–296 (2006)
18. Huq, N.L., Cross, K.J., Ung, M., Reynolds, E.C.: A review of protein structure and gene organisation for proteins associated with mineralised tissue and calcium phosphate stabilisation encoded on human chromosome 4. Arch. Oral Biol. **50**, 599–609 (2005)

19. Fisher, L.W., Torchia, D.A., Fohr, B., Young, M.F., Fedarko, N.S.: Flexible structures of SIBLING proteins, bone sialoprotein, and osteopontin. Biochem. Biophys. Res. Commun. **280**, 460–465 (2001)
20. Bellahcène, A., Castronovo, V., Ogbureke, K.U., Fisher, L.W., Fedarko, N.S.: Small integrin-binding ligand N-linked glycoproteins (SIBLINGs): multifunctional proteins in cancer. Nat. Rev. Cancer **8**, 212–226 (2008)
21. Kawasaki, K., Weiss, K.M.: Mineralized tissue and vertebrate evolution: the secretory calcium-binding phosphoprotein gene cluster. Proc. Natl. Acad. Sci. U.S.A. **100**, 4060–4065 (2003)
22. Fisher, L.W., Fedarko, N.S.: Six genes expressed in bones and teeth encode the current members of the SIBLING family of proteins. Connect. Tissue Res. **44**(Suppl 1), 33–40 (2003)
23. Wright, P.E., Dyson, H.J.: Intrinsically unstructured proteins: re-assessing the protein structure-function paradigm. J. Mol. Biol. **293**, 321–331 (1999)
24. Ward, J.J., Sodhi, J.S., McGuffin, L.J., Buxton, B.F., Jones, D.T.: Prediction and functional analysis of native disorder in proteins from the three kingdoms of life. J. Mol. Biol. **337**, 635–645 (2004)
25. Radivojac, P., Iakoucheva, L.M., Oldfield, C.J., Obradovic, Z., Uversky, V.N., Dunker, A.K.: Intrinsic disorder and functional proteomics. Biophys. J. **92**, 1439–1456 (2007)
26. Romero, P.R., Zaidi, S., Fang, Y.Y., Uversky, V.N., Radivojac, P., Oldfield, C.J., Cortese, M.S., Sickmeier, M., LeGall, T., Obradovic, Z., Dunker, A.K.: Alternative splicing in concert with protein intrinsic disorder enables increased functional diversity in multicellular organisms. Proc. Natl. Acad. Sci. U.S.A. **103**, 8390–8395 (2006)
27. Liu, J., Faeder, J.R., Camacho, C.J.: Toward a quantitative theory of intrinsically disordered proteins and their function. Proc. Natl. Acad. Sci. U.S.A. **106**, 19819–19823 (2009)
28. Boehr, D.D., Nussinov, R., Wright, P.E.: The role of dynamic conformational ensembles in biomolecular recognition. Nat. Chem. Biol. **5**, 789–796 (2009)
29. Lange, O.F., Lakomek, N.A., Farès, C., Schröder, G.F., Walter, K.F., Becker, S., Meiler, J., Grubmüller, H., Griesinger, C., de Groot, B.L.: Recognition dynamics up to microseconds revealed from an RDC-derived ubiquitin ensemble in solution. Science **320**, 1471–1475 (2008)
30. Goobes, G., Goobes, R., Schueler-Furman, O., Baker, D., Stayton, P.S., Drobny, G.P.: Folding of the C-terminal bacterial binding domain in statherin upon adsorption onto hydroxyapatite crystals. Proc. Natl. Acad. Sci. U.S.A. **103**, 16083–16088 (2006)
31. Long, J.R., Dindot, J.L., Zebroski, H., Kiihne, S., Clark, R.H., Campbell, A.A., Stayton, P.S., Drobny, G.P.: A peptide that inhibits hydroxyapatite growth is in an extended conformation on the crystal surface. Proc. Natl. Acad. Sci. U.S.A. **95**, 12083–12087 (1998)
32. Goobes, R., Goobes, G., Shaw, W.J., Drobny, G.P., Campbell, C.T., Stayton, P.S.: Thermodynamic roles of basic amino acids in statherin recognition of hydroxyapatite. Biochemistry **46**, 4725–4733 (2007)
33. Long, J.R., Shaw, W.J., Stayton, P.S., Drobny, G.P.: Structure and dynamics of hydrated statherin on hydroxyapatite as determined by solid-state NMR. Biochemistry **40**, 15451–15455 (2001)
34. Schwartz, S.S., Hay, D.I., Schluckebier, S.K.: Inhibition of calcium phosphate precipitation by human salivary statherin: structure-activity relationships. Calcif. Tissue Int. **50**, 511–517 (1992)
35. Tanabe, T., Fukae, M., Uchida, T., Shimizu, M.: The localization and characterization of proteinases for the initial cleavage of porcine amelogenin. Calcif. Tissue Int. **51**, 213–217 (1992)
36. Yamakoshi, Y., Tanabe, T., Fukae, M., Shimizu, M.: Porcine amelogenins. Calcif. Tissue Int. **54**, 69–75 (1994)
37. Kwak, S.Y., Wiedemann-Bidlack, F.B., Beniash, E., Yamakoshi, Y., Simmer, J.P., Litman, A., Margolis, H.C.: Role of 20-kDa amelogenin (P148) phosphorylation in calcium phosphate formation in vitro. J. Biol. Chem. **284**, 18972–18979 (2009)
38. He, G., Dahl, T., Veis, A., George, A.: Dentin matrix protein 1 initiates hydroxyapatite formation in vitro. Connect. Tissue Res. **44**(Suppl 1), 240–245 (2003)
39. He, G., Dahl, T., Veis, A., George, A.: Nucleation of apatite crystals in vitro by self-assembled dentin matrix protein 1. Nat. Mater. **2**, 552–558 (2003)

40. He, G., Gajjeraman, S., Schultz, D., Cookson, D., Qin, C., Butler, W.T., Hao, J., George, A.: Spatially and temporally controlled biomineralization is facilitated by interaction between self-assembled dentin matrix protein 1 and calcium phosphate nuclei in solution. Biochemistry **44**, 16140–16148 (2005)
41. Gajjeraman, S., Narayanan, K., Hao, J., Qin, C., George, A.: Matrix macromolecules in hard tissues control the nucleation and hierarchical assembly of hydroxyapatite. J. Biol. Chem. **282**, 1193–1204 (2007)
42. Price, P.A., Lim, J.E.: The inhibition of calcium phosphate precipitation by fetuin is accompanied by the formation of a fetuin-mineral complex. J. Biol. Chem. **278**, 22144–22152 (2003)
43. Schafer, C., Heiss, A., Schwarz, A., Westenfeld, R., Ketteler, M., Floege, J., Muller-Esterl, W., Schinke, T., Jahnen-Dechent, W.: The serum protein alpha 2-Heremans-Schmid glycoprotein/fetuin-A is a systemically acting inhibitor of ectopic calcification. J. Clin. Invest. **112**, 357–366 (2003)
44. Holt, C., Wahlgren, N.M., Drakenberg, T.: Ability of a beta-casein phosphopeptide to modulate the precipitation of calcium phosphate by forming amorphous dicalcium phosphate nanoclusters. Biochem. J. **314**, 1035–1039 (1996)
45. Holt, C., Timmins, P.A., Errington, N., Leaver, J.: A core-shell model of calcium phosphate nanoclusters stabilized by beta-casein phosphopeptides, derived from sedimentation equilibrium and small-angle X-ray and neutron-scattering measurements. Eur. J. Biochem. **252**, 73–78 (1998)
46. Holt, C., Sørensen, E.S., Clegg, R.A.: Role of calcium phosphate nanoclusters in the control of calcification. FEBS J. **276**, 2308–2323 (2009)
47. Bar-Yosef Ofir, P., Govrin-Lippman, R., Garti, N., Furedi-Milhofer, H.: The influence of polyelectrolytes on the formation and phase transformation of amorphous calcium phosphate. Cryst. Growth Des. **4**, 177–183 (2004)
48. Tarasevich, B.J., Howarda, C.J., Larsona, J.L., Sneadb, M.L., Simmerc, J.P., Paineb, M., Shawa, W.J.: The nucleation and growth of calcium phosphate by amelogenin. J. Cryst. Growth **304**, 407–415 (2007)
49. Beniash, E., Simmer, J.P., Margolis, H.C.: The effect of recombinant mouse amelogenins on the formation and organization of hydroxyapatite crystals in vitro. J. Struct. Biol. **149**, 182–190 (2005)
50. Wang, L., Guan, X., Du, C., Moradian-Oldak, J., Nancollas, G.H.: Amelogenin promotes the formation of elongated apatite microstructures in a controlled crystallization system. J. Phys. Chem. C, Nanomater Interfaces **111**, 6398–6404 (2007)
51. Liu, X.Y., Lim, S.W.: Templating and supersaturation-driven anti-templating: principles of biomineral architecture. J. Am. Chem. Soc. **125**, 888–895 (2003)
52. Jiang, H., Liu, X.Y., Zhang, G., Li, Y.: Kinetics and template nucleation of self-assembled hydroxyapatite nanocrystallites by chondroitin sulfate. J. Biol. Chem. **280**, 42061–42066 (2005)
53. Yang, X., Wang, L., Qin, Y., Sun, Z., Henneman, Z.J., Moradian-Oldak, J., Nancollas, G.H.: How amelogenin orchestrates the organization of hierarchical elongated microstructures of apatite. J. Phys. Chem. B **114**, 2293–2300 (2010)
54. Fu, G., Qiu, S.R., Orme, C.A., Morse, D.E., De Yoreo, J.J.: Acceleration of calcite kinetics by abalone nacre proteins. Adv. Mater. **17**, 2678–2683 (2005)
55. Elhadj, S., Salter, E.A., Wierzbicki, A., De Yoreo, A.A., Han, N., Dove, P.M.: Peptide controls on calcite mineralization: polyaspartate chain length affects growth kinetics and acts as a stereochemical switch on morphology. Cryst. Growth Des. **6**, 197–201 (2006)
56. Elhadj, S., De Yoreo, J.J., Hoyer, J.R., Dove, P.M.: Role of molecular charge and hydrophilicity in regulating the kinetics of crystal growth. Proc. Natl. Acad. Sci. U.S.A. **103**, 19237–19242 (2006)
57. Michenfelder, M., Fu, G., Lawrence, C., Weaver, J.C., Wustman, B.A., Taranto, L., Evans, J.S., Morse, D.E.: Characterization of two molluscan crystal-modulating biomineralization proteins and identification of putative mineral binding domains. Biopolymers **70**, 522–533 (2003)

58. Qiu, S.R., Wierzbicki, A., Orme, C.A., Cody, A.M., Hoyer, J.R., Nancollas, G.H., Zepeda, S., De Yoreo, J.J.: Molecular modulation of calcium oxalate crystallization by osteopontin and citrate. Proc. Natl. Acad. Sci. U.S.A. **101**, 1811–1815 (2004)
59. Grohe, B., O'Young, J., Ionescu, D.A., Lajoie, G., Rogers, K.A., Karttunen, M., Goldberg, H.A., Hunter, G.K.: Control of calcium oxalate crystal growth by face-specific adsorption of an osteopontin phosphopeptide. J. Am. Chem. Soc. **129**, 14946–14951 (2007)
60. O'Young, J., Chirico, S., Al Tarhuni, N., Grohe, B., Karttunen, M., Goldberg, H.A., Hunter, G.K.: Phosphorylation of osteopontin peptides mediates adsorption to and incorporation into calcium oxalate crystals. Cells Tissues Organs **189**, 51–55 (2009)
61. Hunter, G.K., Grohe, B., Jeffrey, S., O'Young, J., Sørensen, E.S., Goldberg, H.A.: Role of phosphate groups in inhibition of calcium oxalate crystal growth by osteopontin. Cells Tissues Organs **189**, 44–50 (2009)
62. Langdon, A., Wignall, G.R., Rogers, K., Sørensen, E.S., Denstedt, J., Grohe, B., Goldberg, H.A., Hunter, G.K.: Kinetics of calcium oxalate crystal growth in the presence of osteopontin isoforms: an analysis by scanning confocal interference microcopy. Calcif. Tissue Int. **84**, 240–248 (2009)
63. Jung, T., Sheng, X., Choi, C.K., Kim, W.S., Wesson, J.A., Ward, M.D.: Probing crystallization of calcium oxalate monohydrate and the role of macromolecule additives with in situ atomic force microscopy. Langmuir **20**, 8587–8596 (2004)
64. Iijima, M., Moradian-Oldak, J.: Interactions of amelogenins with octacalcium phosphate crystal faces are dose dependent. Calcif. Tissue Int. **74**, 522–531 (2004)
65. Iijima, M., Moradian-Oldak, J.: Control of octacalcium phosphate and apatite crystal growth by amelogenin matrices. J. Mater. Chem. **14**, 2189–2199 (2004)
66. Tsuji, T., Onuma, K., Yamamoto, A., Iijima, M., Shiba, K.: Direct transformation from amorphous to crystalline calcium phosphate facilitated by motif-programmed artificial proteins. Proc. Natl. Acad. Sci. U.S.A. **105**, 16866–16870 (2008)
67. Onuma, K., Oyane, A., Tsutsui, K., Tanaka, K., Treboux, G., Kanzaki, N., Ito, A.: Precipitation kinetics of hydroxyapatite revealed by the continuous-angle laser light-scattering technique. J. Phys. Chem. B **104**, 10563–10568 (2000)
68. Tsuji, T., Onimaru, M., Yanagawa, H.: Towards the creation of novel proteins by block shuffling. Comb. Chem. High Throughput Screen. **9**, 259–269 (2006)
69. Shiba, K.: Molcraft a hierarchical approach to the synthesis of artificial proteins. J. Mol. Catal. B. **28**, 145–153 (2004)
70. Shiba, K.: Natural and artificial peptide motifs: their origins and the application of motif-programming. Chem. Soc. Rev. **39**, 117–126 (2009)
71. Saito, H., Honma, T., Minamisawa, T., Yamazaki, K., Noda, T., Yamori, T., Shiba, K.: Synthesis of functional proteins by mixing peptide motifs. Chem. Biol. **11**, 765–773 (2004)
72. Simmer, J.P., Hu, J.C.: Expression, structure, and function of enamel proteinases. Connect. Tissue Res. **43**, 441–449 (2002)
73. Tao, J., Pan, H., Zeng, Y., Xu, X., Tang, R.: Roles of amorphous calcium phosphate and biological additives in the assembly of hydroxyapatite nanoparticles. J. Phys. Chem. B **111**, 13410–13418 (2007)
74. Banfield, J.F., Welch, S.A., Zhang, H., Ebert, T.T., Penn, R.L.: Aggregation-based crystal growth and microstructure development in natural iron oxyhydroxide biomineralization products. Science **289**, 751–754 (2000)
75. Scott, J.K., Smith, G.P.: Searching for peptide ligands with an epitope library. Science **249**, 386–390 (1990)
76. Boder, E.T., Wittrup, K.D.: Yeast surface display for screening combinatorial polypeptide libraries. Nat. Biotechnol. **15**, 553–557 (1997)
77. Hanes, J., Plückthun, A.: In vitro selection and evolution of functional proteins by using ribosome display. Proc. Natl. Acad. Sci. U.S.A. **94**, 4937–4942 (1997)
78. Keefe, A.D., Szostak, J.W.: Functional proteins from a random-sequence library. Nature **410**, 715–718 (2001)

79. Tsuji, T., Onimaru, M., Doi, N., Miyamoto-Sato, E., Takashima, H., Yanagawa, H.: In vitro selection of GTP-binding proteins by block shuffling of estrogen-receptor fragments. Biochem. Biophys. Res. Commun. **390**, 689–693 (2009)
80. Sarikaya, M., Tamerler, C., Jen, A.K., Schulten, K., Baneyx, F.: Molecular biomimetics: nanotechnology through biology. Nat. Mater. **2**, 577–585 (2003)
81. Brown, S.: Metal-recognition by repeating polypeptides. Nat. Biotechnol. **15**, 269–272 (1997)
82. Brown, S., Sarikaya, M., Johnson, E.: A genetic analysis of crystal growth. J. Mol. Biol. **299**, 725–735 (2000)
83. Whaley, S.R., English, D.S., Hu, E.L., Barbara, P.F., Belcher, A.M.: Selection of peptides with semiconductor binding specificity for directed nanocrystal assembly. Nature **405**, 665–668 (2000)
84. Mao, C., Flynn, C.E., Hayhurst, A., Sweeney, R., Qi, J., Georgiou, G., Iverson, B., Belcher, A.M.: Viral assembly of oriented quantum dot nanowires. Proc. Natl. Acad. Sci. U.S.A. **100**, 6946–6951 (2003)
85. Lee, Y.J., Yi, H., Kim, W.J., Kang, K., Yun, D.S., Strano, M.S., Ceder, G., Belcher, A.M.: Fabricating genetically engineered high-power lithium-ion batteries using multiple virus genes. Science **324**, 1051–1055 (2009)
86. Gungormus, M., Fong, H., Kim, I.W., Evans, J.S., Tamerler, C., Sarikaya, M.: Regulation of in vitro calcium phosphate mineralization by combinatorially selected hydroxyapatite-binding peptides. Biomacromolecules **9**, 966–973 (2008)
87. Roy, M.D., Stanley, S.K., Amis, E.J., Becker, M.L.: Identification of a highly specific hydroxyapatite-binding peptide using phage display. Adv. Mater. **20**, 1830–1836 (2008)
88. Sano, K., Shiba, K.: A hexapeptide motif that electrostatically binds to the surface of titanium. J. Am. Chem. Soc. **125**, 14234–14235 (2003)
89. Kashiwagi, K., Tsuji, T., Shiba, K.: Directional BMP-2 for functionalization of titanium surfaces. Biomaterials **30**, 1166–1175 (2009)
90. Tsuji, T., Oaki, Y., Yoshinari, M., Kato, T., Shiba, K.: Motif-programmed artificial proteins mediated nucleation of octacalcium phosphate on the titanium substrates. Chem. Commun. **46**, 6675–6677 (2010)